Original Article

Comprehensive analysis of molecular characteristics between primary and breast-derived metastatic ovarian cancer

Junqi Long[1#], Bo Liu[2#], Jinmeng Li[1#], Xinchan Ji[1], Nian Zhu[1], Xujie Zhuang[1], Huina Wang[1], Lujia Li[1], Yuhaoran Chen[1], Xiaohui Li[3], Shuangtao Zhao[4]^

[1]School of Software Engineering, Faculty of Information Technology, Beijing University of Technology, Beijing, China; [2]School of Mathematical and Computational Sciences, Massey University, Auckland, New Zealand; [3]Department of Joint Surgery, Tianjin Hospital, Tianjin University, Tianjin, China; [4]Department of Thoracic Surgery, Beijing Tuberculosis and Thoracic Tumor Research Institute/Beijing Chest Hospital, Capital Medical University, Beijing, China

Contributions: (I) Conception and design: S Zhao; (II) Administrative support: None; (III) Provision of study materials or patients: None; (IV) Collection and assembly of data: J Long, J Li; (V) Data analysis and interpretation: J Long, B Liu; (VI) Manuscript writing: All authors; (VII) Final approval of manuscript: All authors.

[#]These authors contributed equally to this work.

Correspondence to: Xiaohui Li, MD. Department of Joint Surgery, Tianjin Hospital, Tianjin University, 406 Jiefang North Road, Tianjin 300211, China. Email: lxhchd@sina.com; Shuangtao Zhao, MD, PhD. Department of Thoracic Surgery, Beijing Tuberculosis and Thoracic Tumor Research Institute/Beijing Chest Hospital, Capital Medical University, 9 Beiguan Street Yard, Beijing 101149, China. Email: zst-1981@163.com.

Background: The molecular basis for the disparities between primary ovarian cancer (POC) and ovarian cancer secondary to breast cancer (OCSTBC) remains poorly understood. This study aimed to explore the different characteristics between them through genomic analysis.

Methods: We performed differentially expressed genes (DEGs) analysis between POC (n=96) and OCSTBC (n=44) groups with transcriptome data and revealed the enriched biological pathways with Kyoto Encyclopedia of Genes and Genomes (KEGG) and Hallmark gene sets between these two groups. Then, the Microenvironment Cell Populations (MCP)-counter and Cell-type Identification by Estimating Relative Subsets of RNA Transcript (CIBERSORT) algorithms were applied to evaluate the immune infiltration in tumor microenvironment (TME) between them. Finally, we performed the association analysis within single nucleotide polymorphism (SNP) data and obtained some meaningful SNPs and candidate genes for further transcriptomic analysis.

Results: We identified a total of 13 cancer-related genes including *GATA3*, *FOXA1*, *CCND1*, and *TTK* between POC (n=96) and OCSTBC (n=44) groups with DEGs analysis. Integrated analysis revealed more significant immune-enriched pathways in the POC than in the OCSTBC group. Most immune cells had higher infiltration abundance in POC, except M2 macrophages, which was higher in OCSTBC. In SNP analysis, four SNP regions (8q12.1, 11q21, 11q24.3, and 17q25.3) were found to be significantly correlated with phenotypes (POC/OCSTBC), and importantly, some new susceptibility genes such as *ETS1*, *CWC15*, and *XKR4* were revealed to potentially be associated with distinction between POC and OCSTBC.

Conclusions: Our study provides a systematic molecular characteristic between POC and OCSTBC and suggests a pressing need to develop some specific therapeutic strategies in certain types of ovarian cancer.

Keywords: Breast cancer; metastasis; primary ovarian cancer (POC); genes

Submitted Aug 17, 2024. Accepted for publication Jan 14, 2025. Published online Mar 24, 2025.
doi: 10.21037/tcr-24-1441
View this article at: https://dx.doi.org/10.21037/tcr-24-1441

^ ORCID: 0000-0002-8624-7834.

Introduction

Background

Ovarian cancer is the most dangerous type of cancer among gynecological tumors (1-4). Some 70% of ovarian cancer patients have already reached an advanced stage by diagnosis. The 5-year survival rate of ovarian cancer is about 30% (5). Metastatic ovarian cancer is a malignant tumor that spreads from a primary tumor outside the ovary to the ovary (3,6,7). According to statistics, metastatic ovarian tumors account for about 8% of ovarian tumor surgeries (8). The mammary gland and gastrointestinal tract are the most common primary sites of secondary ovarian disease (6,9-14). Ovarian tumors that metastasize from the breast to the ovary account for 3–38% of all ovarian tumors (9,10). Patients with a history of breast cancer are 3–7 times more likely to develop primary than secondary ovarian cancers (9,10). Multiple studies have shown that ovarian cancer that spreads from the breast to the ovary is usually asymptomatic in its early stages and is not diagnosed until the tumor has grown to a certain size (8-10,15-17). This tumor usually presents as a bilateral, solid, and small ovarian mass (8-10,15-17).

Highlight box

Key findings

- Our study provides a systematic molecular characteristic between primary ovarian cancer (POC) and ovarian cancer secondary to breast cancer (OCSTBC).

What is known and what is new?

- According to clinical and histological studies, OCSTBC mimics the characteristics of POC, but the treatment and prognosis of the two are different. Therefore, it is crucial to distinguish OCSTBC from POC.
- Our results provided some complementary information to enhance understanding of ovarian cancer with different clinical stages and a panoramic view of the altered cancer genome and signaling pathways between POC and OCSTBC groups.

What is the implication, and what should change now?

- With a clearer molecular distinction between POC and OCSTBC, healthcare providers can tailor treatments more precisely based on the specific type of cancer, potentially improving outcomes for patients.
- Changes should be made in diagnostic protocols to include molecular profiling as part of the standard workup for ovarian cancer. The development of targeted therapies or adjustments to existing treatment regimens should be made based on the molecular characteristics identified.

Rationale and knowledge gap

According to clinical and histological studies, ovarian cancer secondary to breast cancer (OCSTBC) mimics the characteristics of primary ovarian cancer (POC) (9,18-23). As a result, it is difficult to distinguish between these two diseases; however, the treatment and prognosis of the two groups of tumors are different. Secondary ovarian cancer has a poor prognosis, with a survival of 9–30 months. Patients with POC have a longer survival, with a median progression-free survival of 20–40 months (9,15,24). Therefore, it is crucial to distinguish OCSTBC from POC.

Objective

Our research aimed to discover the molecular characteristics for distinguishing between POC and OCSTBC through computational medical analysis. We present this article in accordance with the STREGA reporting checklist (available at https://tcr.amegroups.com/article/view/10.21037/tcr-24-1441/rc).

Methods

Data source

The clinical and genomic data of ovarian cancer patients (GSE20565) (25) was downloaded from Gene Expression Omnibus (GEO, https://www.ncbi.nlm.nih.gov/geo) database. We extracted the transcriptome data of 44 patients with OCSTBC and 96 patients with POC, as well as the single nucleotide polymorphism (SNP) data of 15 patients with secondary ovarian cancer and POC. The detailed clinical information of patients enrolled in this study are presented in Table S1. The entire analysis flow is displayed in *Figure 1*. The study was conducted in accordance with the Declaration of Helsinki (as revised in 2013).

Identification of differentially expressed genes (DEGs) and enriched signaling pathways

Before differential analysis, we extracted a list of tumor-specific genes. The list was generated based on the DEGs of GSE38666 (26) and the gene expression profile of normal ovaries in the Human Protein Atlas (HPA, https://www.proteinatlas.org/) (Figure S1).

The "limma" (27) R package was used to screen DEGs between POC and OCSTBC. A cut-off of gene expression fold change of ≥2 or ≤–2 and false discovery rate (FDR)

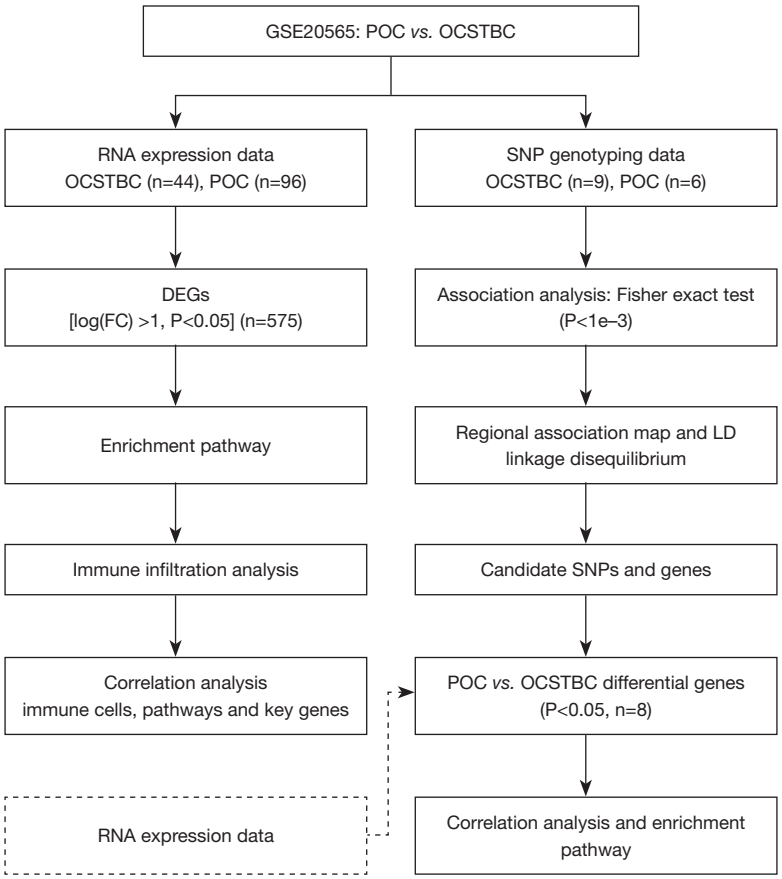

Figure 1 The flow chart of this study. POC, primary ovarian cancer; OCSTBC, ovarian cancer secondary to breast cancer; DEGs, differentially expressed genes; LD, linkage disequilibrium; SNP, single nucleotide polymorphism; FC, fold change.

q-value of <0.05 was applied to obtain the most significant DEGs, which were enriched into pathways according to the Molecular Signatures Database (MSigDB, https://www.gsea-msigdb.org/gsea/msigdb) (28). Signaling pathways with FDR P<0.05 were considered statistically significant.

Immune infiltration analysis of transcriptome data

Microenvironment Cell Populations (MCP)-counter (29) and Cell-type Identification by Estimating Relative Subsets of RNA Transcript (CIBERSORT) (30) R packages were applied to perform immune infiltration analysis on the original expression data of the transcriptome. MCP-counter was used to compute the absolute abundance scores for 10 cell types, and the CIBERSORT algorithm was used to estimate the relative cellular fraction of 22 immune cell types. The immune profiles were performed with a hierarchical clustering and compared between POC and OCSTBC.

Association analysis with SNP data

A total of 58,391 SNP sites were enrolled into the SNP data from 15 patients including POC (n=6) and OCSTBC (n=9). The SNPs with a deletion rate greater than 10% were filtered out, and we deleted the SNPs with minor allele frequency (MAF) and SNPs that deviated from Hardy-Weinberg equilibrium (HWE). Finally, we performed further study with the remaining 38,677 SNPs.

We performed association analysis in "Plink" software (31). These 15 samples were divided into POC (n=6, Control) and OCSTBC (n=9, Case) groups. After the quality control process, "Plink" was used to carry out the Fisher's exact test of alleles, and the R software package "qqman" (32) was used to visualize the results as Manhattan plots. Then, the software "Plink" was used to calculate the r^2

matrix between the 200 kb upstream and downstream SNPs of the candidate SNP, and the R package "LDheatmap" (33) was used to visualize the r^2 matrix in the haploid block. We used "LocusZoom" (34) tool to show the 200 kb genomic region upstream and downstream of the candidate SNP in detail.

Correlation analysis

To explore the relationship among the key genes, pathways, and immune cells, we used the $\log_2$ standardized gene expression matrix as an input data to perform gene set variation analysis (GSVA) (35). Then, we calculated the Pearson correlation coefficients between pathways and immune cells based on a score matrix within 140 samples in 56 pathways. Meanwhile, we conducted a similar process between key genes and immune cells with differences in infiltration. The tool Cytoscape (36) was used to visualize the network diagram.

Statistical analysis

In addition to the methods listed above, all the other statistical analyses were performed in R statistical environment. Statistical significance of differences was produced by *t*-test when comparing continuous variables, Fisher's exact test when comparing frequencies, and limma when comparing genomic differences. All P values were derived from two-tailed tests. Benjamini-Hochberg method was applied to control the FDR and correct P value for multiple testing. The statistical significance of an FDR adjusted P value (or q-value) was defined as 0.05.

Results

Identify DEGs and significant enrichment pathways between POC and OCSTBC

To investigate the genomic differences between the POC and OCSTBC groups, we detected a total of 6,191 ovarian tumor-specific genes in all samples (n=140) enrolled into this study, of which 575 DEGs were identified between POC and OCSTBC (Table S2). As a result, we discovered that some of the functionally well characterized genes associated with metastasis exhibited significantly variable abundance in OCSTBC, such as *GATA3*, *FOXA1*, *MYB*, *CCND1*, and *SOX9*. Meanwhile *TTK*, *FOXA2*, *BIRC3*, *IL32*, *MET*, *CDKN2A*, *CXCR4*, and *MYCL* were shown to be significantly enriched in the primary group (*Figure 2A-2C*, Figure S2). Especially, the DEGs distribution was balanced between OCSTBC and POC except for *GATA3* [P<0.001, $\log_2$ fold change ($\log_2$FC) =7.980] and *FOXA1* (P<0.001, $\log_2$FC =7.130) with notable significance (*Figure 2A*).

To further understand the molecular function of these highly abundant genes, we performed pathway enrichment analysis to explore dysregulated molecular processes informed by the genomics data. A total of 45 upregulated Hallmark and Kyoto Encyclopedia of Genes and Genomes (KEGG) pathways were identified which were predominantly composed of cell cycle and oncogenic signaling (*Figure 2D*) in the POC group, such as E2F targets, G2M checkpoint, and KRAS signaling upregulation. However, a total of 12 significant Reactome and Hallmark pathways correlated with cancer invasion and metastasis (37,38) were discovered to be enriched in OCSTBC group, including interleukin 7 signaling, estrogen-dependent gene expression, nuclear receptors signaling, and ESR-mediated signaling (*Figure 2E*). Especially, *CCND1*, *CXCR4*, and *CDKN2A* were enriched in more pathways with high expression value (*Figure 2F*).

Deconvolution of the cellular composition of tumor samples revealed immune-associated tumor microenvironment (TME) between POC and OCSTBC

To investigate the TME including cytokine, growth factors, and cellular components that promote tumor development, we performed immune infiltration analysis with two deconvolution approaches—MCP-counter (29) to compute absolute abundance scores of 10 immune-related cell types (*Figure 3A*,*3B*, Figure S3), and CIBERSORT (30) to evaluate the relative cellular fraction for 22 immune cell types (*Figure 3C*,*3D*). Supervised clustering of the abundance scores of the biomarkers for each cell type classified these samples into two subgroups, and the expression profiles from both clusters presented significantly distinct signatures (*Figure 3B*).

Further, we discovered that the abundance scores stemming from MCP-counter displayed abundance of T cells, $CD8^+$ T cells, cytotoxic lymphocytes, neutrophils, B lineage, monocytic lineage, and myeloid dendritic cells were significantly lower in the OCSTBC group, but significantly higher for endothelial cells and fibroblasts (*Figure 3A*). Interestingly, some biomarkers of neutrophils such as *MEGF9*, *STEAP4*, *TECPR2*, and *TLE3* were

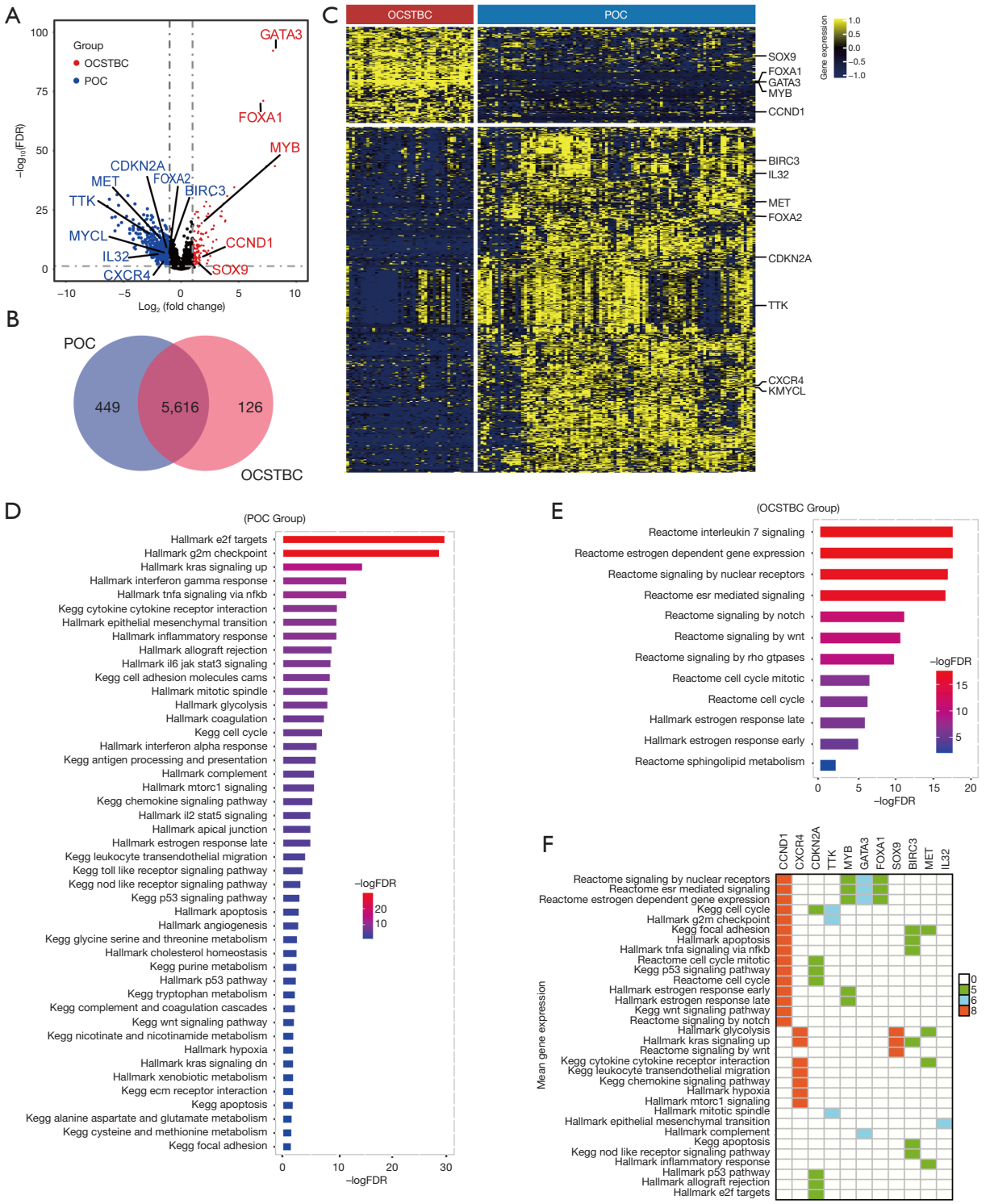

Figure 2 Differential genes and pathways. (A) Volcano plot showing differential analysis of gene expression between POC (blue dots) and OCSTBC (red dots). (B) Venn diagram showing the quantitative relationship of 6,191 genes after differential analysis. (C) Expression of 575 differential genes in POC samples (blue group) and OCSTBC samples (red group). (D,E) Pathway enrichment of two groups of differential genes. (F) Heatmap showing relationships between key genes and pathways. The color represents the mean expression of the gene in all samples. POC, primary ovarian cancer; OCSTBC, ovarian cancer secondary to breast cancer; FDR, false discovery rate.

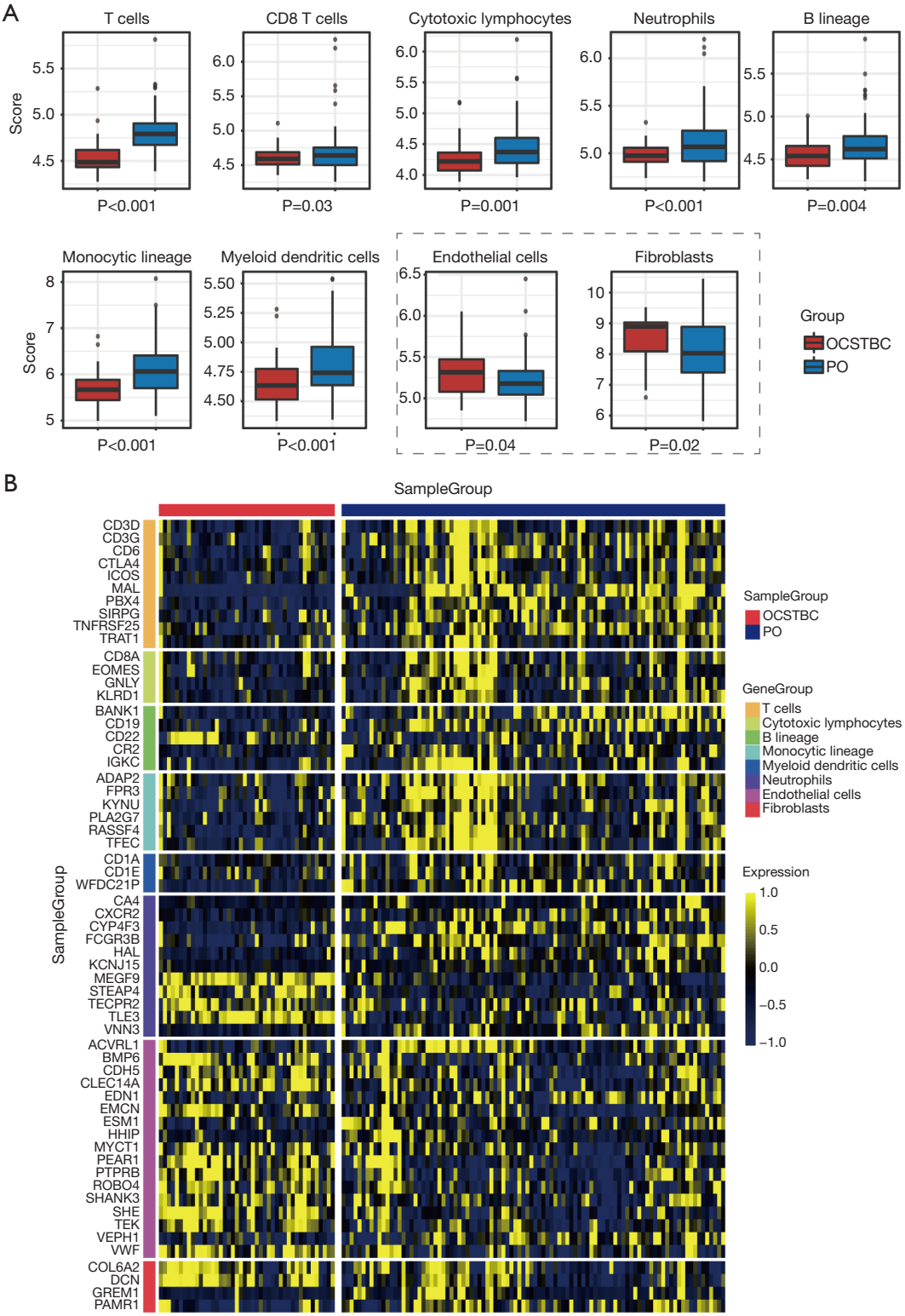

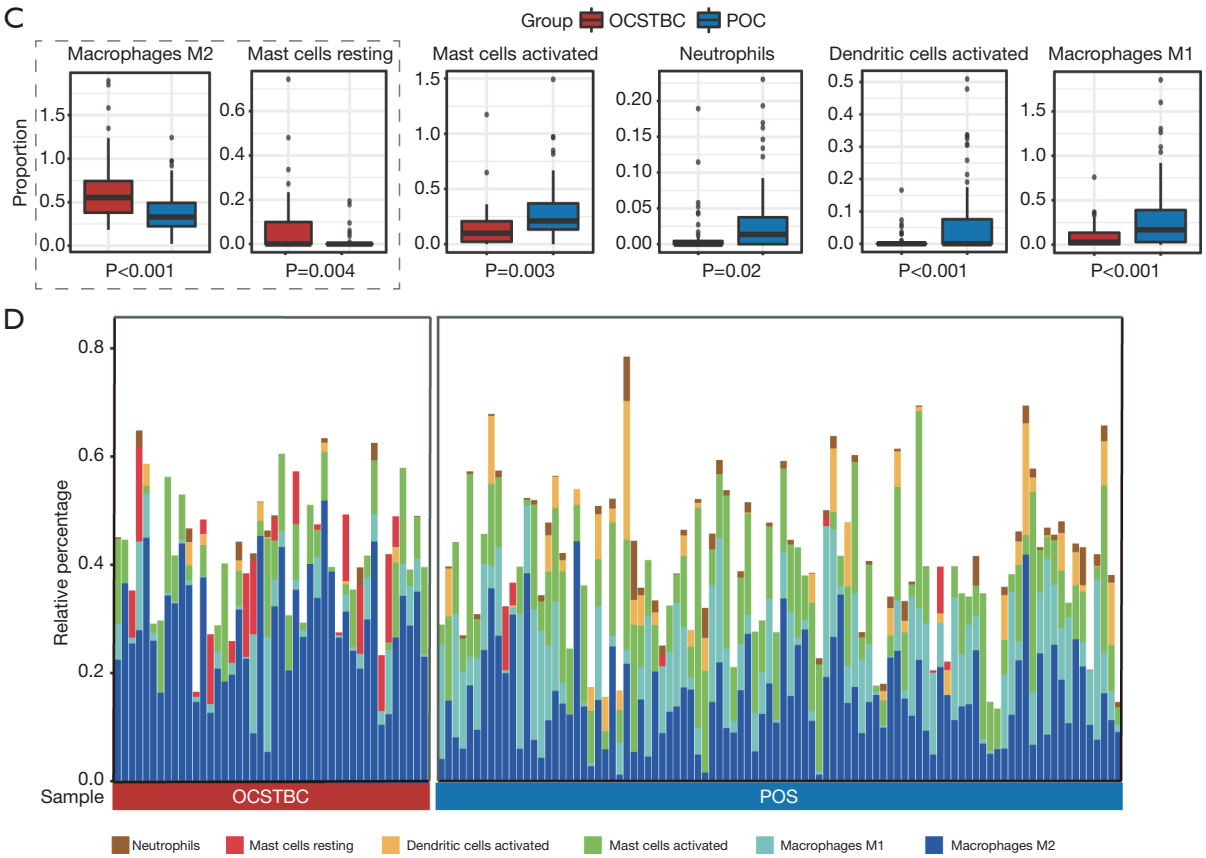

Figure 3 Differences between POC and OCSTBC in the immune environment. (A) Boxplot shows the difference in immune cell (MCP-counter) infiltration between the two groups. (B) Expression of key genes of immune cells (MCP-counter) in POC and OCSTBC samples. (C) Boxplot shows the difference in immune cell (CIBERSORT) infiltration between the two groups. (D) Stacked histogram representing the proportion of cells with differential immune infiltration (CIBERSORT). The abscissa is the sample, and the ordinate is the proportion. MCP, Microenvironment Cell Populations; POC, primary ovarian cancer; OCSTBC, ovarian cancer secondary to breast cancer; CIBERSORT, Cell-type Identification by Estimating Relative Subsets of RNA Transcript.

significantly lower in the POC group (*Figure 3B*). The association analysis combined with previous studies found that *TLE3* benefited from taxane chemotherapy in ovarian cancer (39) and served as an effective indicator for predicting the efficacy of eribulin chemotherapy in triple-negative breast cancer (40), and might have served as a new therapeutic target for OCSTBC. Among 22 inferred immune cell types from CIBERSORT, the cellular fractions of macrophages M2, mast cells resting, mast cells activated, neutrophils, dendritic cells activated, and macrophages M1 varied significantly across the subgroups (*Figure 3C,3D*), especially for the macrophages M2. A higher fraction of macrophages M2 is correlated with a more aggressive tumor characteristic, reflected by tumor invasion, progression, and metastasis (41,42). In agreement with this, M2 infiltration was obviously associated with large tumor size and angiogenesis in breast cancer (43). Also, macrophages M2 could induce chemoresistance by secreting growth factors (44) and lead to therapy failure and poor prognosis in patients. Through comprehensive analysis, it can be concluded that tumor cells might have reconstructed the immune-related TME to facilitate ovarian cancer progression.

Insights into interactions between signaling pathways/driver genes and immune cells in TME

A third frontier involves interactions between signaling pathways/driver genes and immune cells in TME including cancer cells, stromal cells, and the immune infiltrate. To reveal key dysregulated signaling pathways occurring in each immune cell, we calculated the correlation score

between 56 signaling pathways and 9 immune cells for which an oncogenic process was associated with a certain subgroup. With few exceptions (e.g., purine metabolism), general cancer-related processes, such as immune response, oncogenic signaling, cell cycle, DNA repair, metabolic reprogramming, hypoxia, and angiogenesis, were frequently dysregulated between POC and OCSTBC groups. Especially for the POC subgroup, these cancer-related processes were significantly positively correlated with seven major immune cells (P<0.05, *Figure 4A*). However, these dysregulated pathways were significantly positively correlated with endothelial cells and fibroblasts in both POC and OCSTBC subgroups (*Figure 4A*).

Further, we also observed that these driver genes including of *CCND1*, *FOXA1*, *GATA3*, *MYB*, and *SOX9* were significantly negatively correlated with those nine immune cells from MCP-counter, whereas the other driver genes were markedly positively associated with them, such as *BIRC3*, *IL32*, *MET*, *CDKN2A*, *CXCR4*, and so on (P<0.05, *Figure 4B*). Interestingly, the three driver genes (*MYB*, *GATA3*, and *FOXA1*) were positively correlated with macrophages M2 and mast cells resting in the OCSTBC group, and meanwhile, *BIRC3* and *IL32* were positively correlated with the other four immune cells (neutrophils, dendritic cells activated, mast cells activated, and macrophages M1) in CIBERSORT analysis (*Figure 4C*). Obviously, T cells were strongly positively correlated with *BIRC3* and *IL32* (P<0.05, r>0.5) but a strongly negatively associated with *FOXA1* and *GATA3* (P<0.05, r<−0.5), which suggested that these T cells might be converted to regulatory T cells that promote tumor immune escape in target tissues (45,46). Together, these data revealed the significantly different correlation between immune cells and functional signaling pathways/driver genes in OCSTBC patients compared with POC cases.

Association analysis identifies multiple susceptibility loci associated with breast metastasis in ovarian cancer

To identify some new risk factors associated with breast metastases in ovarian cancer, we performed an association study by genotyping 58,391 SNPs in 15 patients with ovarian cancer including of POC (n=6) and OCSTBC (n=9) cases. As a result, a total of 30 SNPs were discovered to be associated with the phenotype (POC/OCSTBC) with a significance threshold of 0.001 (Table S3). Then, we identified six susceptibility loci on chromosomes 5q14.1, 2q32.3, 11q21, 8q12.1, 17q25.3, and 11q24.3 (P<0.001); among of them, four new susceptibility loci were located in *XKR4*, *CWC15*, *PGS1*, and *ETS1*, and two low-frequency variants rs7107185 and rs4128561 had relatively high effect size [odds ratio (OR) >28, *Figure 5A*].

To investigate whether the association with the phenotype (POC/OCSTBC) at each of the four susceptibilities loci above could be completely explained by the index SNP, we performed an imputation analysis for the four regions identified. All these imputed SNPs were subjected to linkage disequilibrium (LD) analysis with genotyping-identified rs7107185, rs4302823, rs4129767, and rs4128561, respectively (*Figure 5B*). Finally, we uncovered that rs7107185 in intron 5 of *CWC15* [OR =33, 95% confidence interval (CI): 4.659–233.764, P<0.001] with high LD (r^2=0.99) was adjacent to rs10501819 in *KDM4D*. In addition, rs10501819 remained significant genome-wide (Figure S4), indicating that rs7107185 may be an independent susceptibility marker. Similarly, our association analysis identified another three SNPs mapping to the regions of chromosomes 8q12.1, 17q25.3, and 11q24.3 (*Figure 5B*). All of them displayed that these SNPs were significantly associated with the phenotype (POC/OCSTBC), which highlighted the involvement of multiple genetic loci in the development of breast-to-ovarian metastasis (*Figure 5B*).

Potential cancer-related genes and dysregulated molecular pathways of ovarian cancer

We further explored transcriptome differences between POC and OCSTBC in 71 candidate genes (Figure S5). We identified that eight candidate genes (*PGS1*, *BIRC5*, *SOCS3*, *CWC15*, *SRSF8*, *ENDOD1*, *XKR4*, and *ETS1*) were significantly upregulated in the POC group compared with the OCSTBC group (*Figure 6A*), which were negatively correlated with the five key genes (*CCND1*, *FOXA1*, *GATA3*, *MYB*, and *SOX9*) in the OCSTBC group but positively associated with the other eight key genes (*BIRC3*, *IL32*, *MET*, *CDKN2A*, *CXCR4*, *FOXA2*, *MYCL*, and *TTK*) in the POC group (*Figure 6B*). Then, we carried out the pathway enrichment analysis to investigate the dysregulated molecular processes informed by the genomic data. A total of 42 upregulated Hallmark and KEGG pathways were identified which were predominantly composed of cancer immune, apoptosis, oncogenic signaling, metabolism and cell cycle, and DNA repair signaling pathways (*Figure 6C*). These data suggested that the protein data provided complementary information to yield an improved

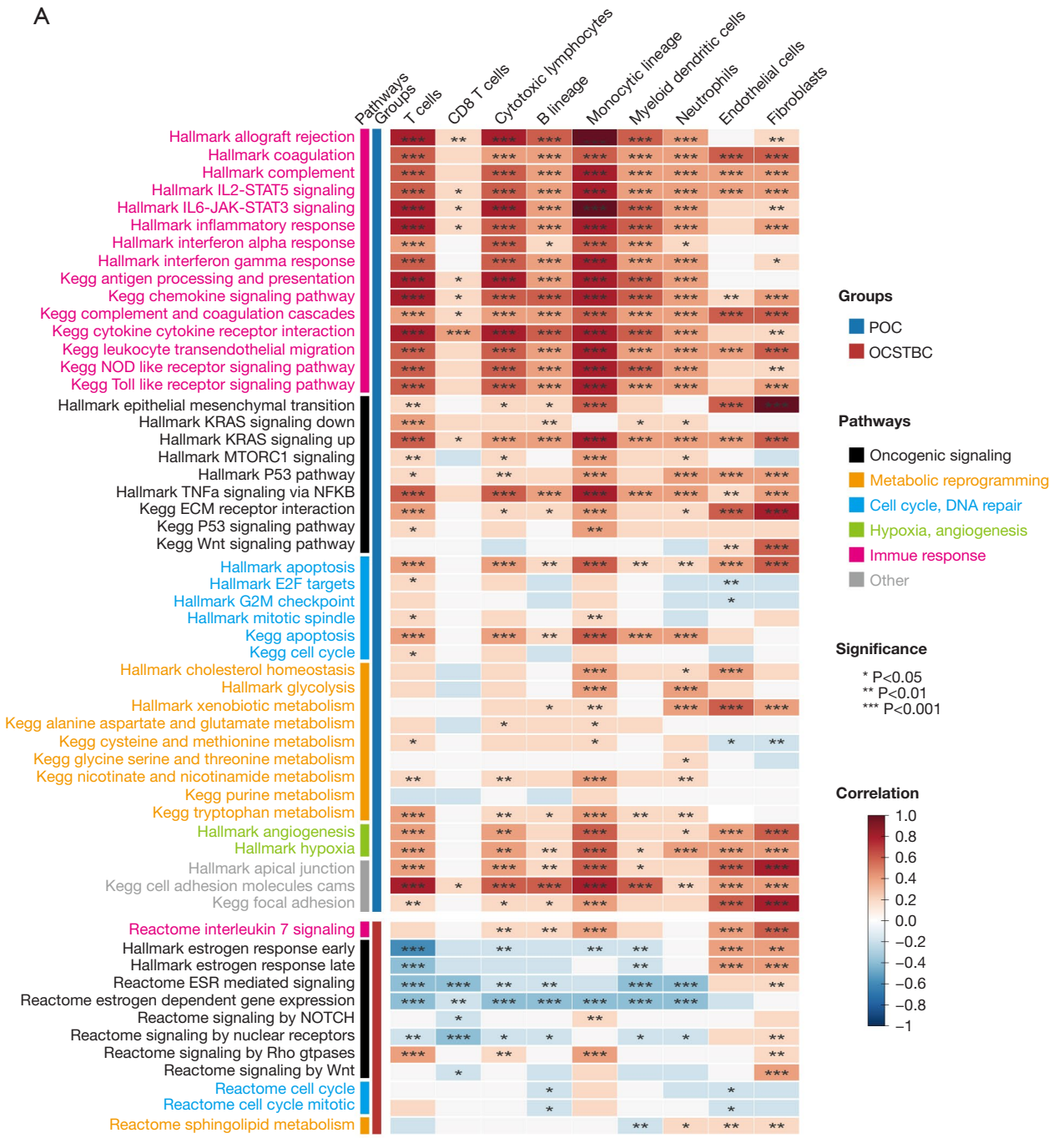

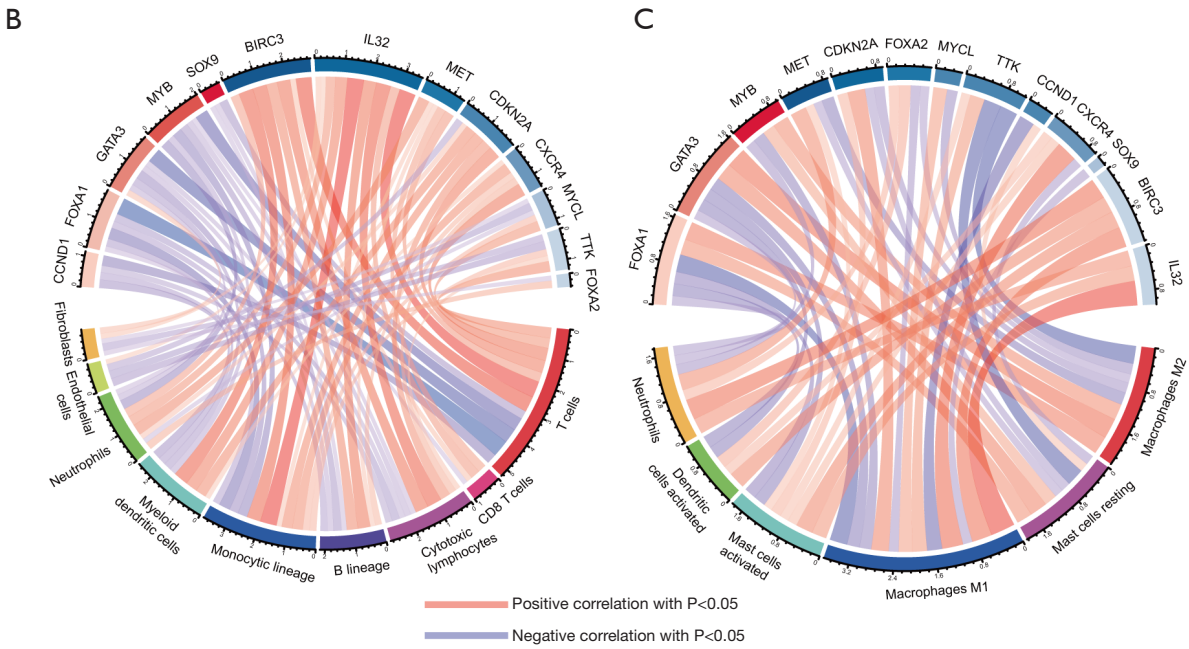

Figure 4 Correlation of the key genes, pathways, and immunity. (A) Correlation between pathways and immune cells (MCP-counter). POC represents the pathways enriched by differential genes of the primary ovarian cancer group, and OCSTBC represents the pathways enriched by differential genes of the ovarian cancer secondary to breast cancer group. Each set of pathways is marked with a different color according to its function. (B) Correlation of key genes with immune cells (MCP-counter). Genes marked in blue are of the primary ovarian cancer group and genes marked in red are of the ovarian cancer secondary to breast cancer group. Red links represent positive correlations and blue links represent negative correlations. The color and width of the lines become darker or wider as the correlation coefficient increases. (C) Correlation between key genes and immune cells (CIBERSORT). MCP, Microenvironment Cell Populations; POC, primary ovarian cancer; OCSTBC, ovarian cancer secondary to breast cancer; CIBERSORT, Cell-type Identification by Estimating Relative Subsets of RNA Transcript; ECM, extracellular matrix.

understanding of biological processes involved in ovarian cancer.

Discussion

Our study aimed to identify the differences in genomics and transcriptome among ovarian cancer patients between POC and OCSTBC groups. Our results provided some complementary information to understand the ovarian cancer with different clinical stages and a panoramic view of the altered cancer genome and signaling pathways between POC and OCSTBC groups.

A large number of significant genes associated with tumor cell enrichment were identified between POC and OCSTBC groups, as might be expected. Oncogenic and cell cycle signaling pathways predominated in the POC group, whereas cancer invasion and metastasis-related pathways were enriched in the OCSTBC group. Thus, patients in the POC group were more representative of genomic expression and pathway alterations with occurrence of key genes including *MET*, *BIRC3*, *TTK*, *MYCL*, and *CDKN2A*. However, the OCSTBC group with higher expression of *SOX9*, *FOXA1*, *GATA3*, *MYB*, and *CCND1* may benefit from alternative therapies that take advantage of predominance of metastasis-related tumor cells. In this study, the expression of *GATA3* and *FOXA1* were significantly upregulated between the two groups, which helps distinguish breast cancer metastasis (47). In addition, a study of cohorts with both breast and ovarian cancer discovered that all POCs were negative for *GATA3*, whereas all breast cancers that metastasized to the ovary showed positive immunoreactivity (48). This phenomenon and our experimental results simultaneously corroborate the specificity of *GATA3* for breast cancer cells. Thus, the high sensitivity and specificity of *GATA3* and *FOXA1* in the breast may help us to distinguish OCSTBC patients in

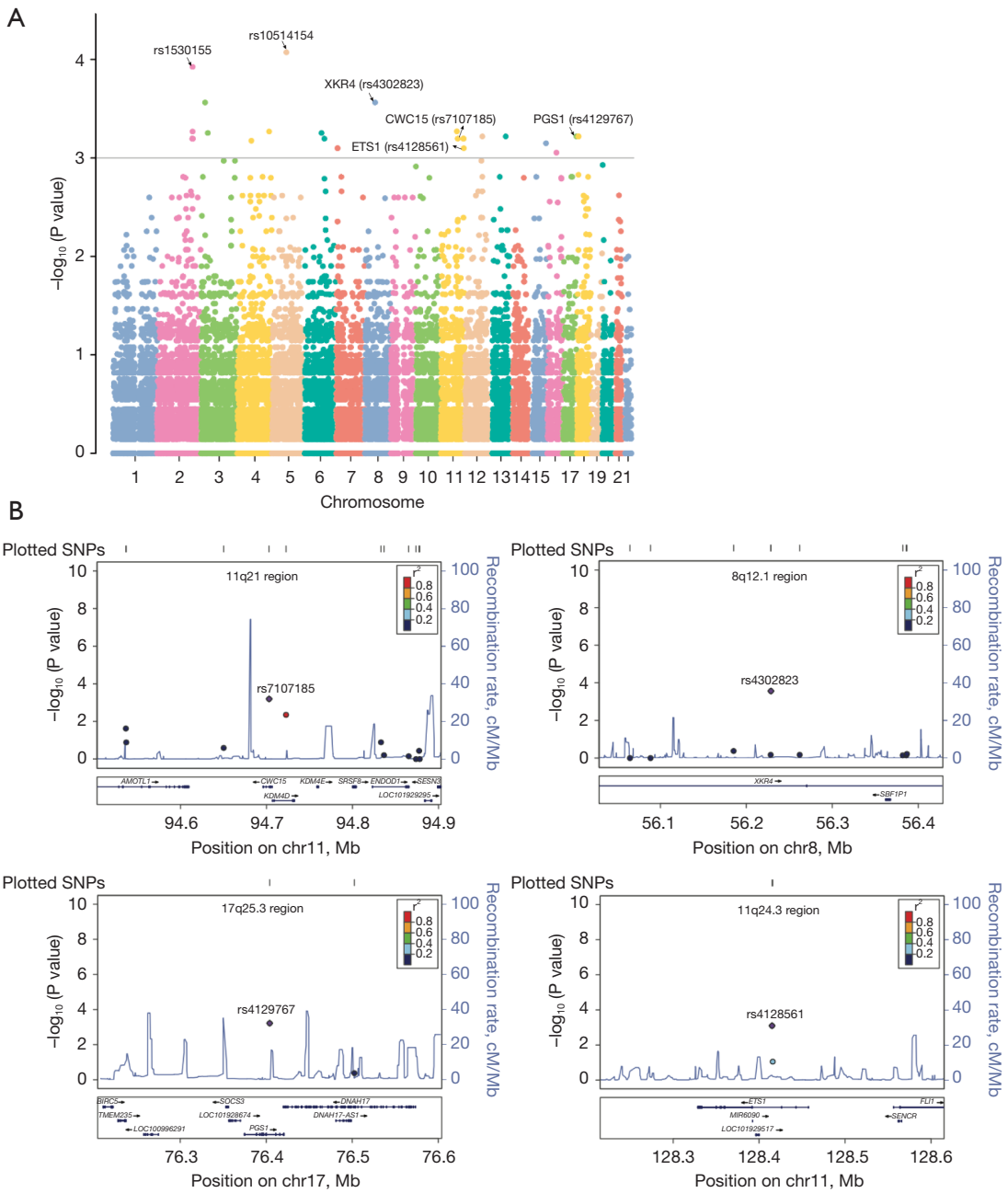

Figure 5 SNP association analysis and candidate genes screening. (A) Manhattan plot shows the results of Fisher's exact test. Each dot represents a SNP site. The grey line represents the relaxed threshold P value <0.001. (B) Regional association map of the 200 kb range around the 4 candidate SNPs. Dots indicate the chromosomal location of the SNP site and its significance [$-\log_{10}$(P value)]. The color of the dots indicates the intensity of the LD. The blue lines represent the recombination rate. LD, linkage disequilibrium; SNP, single nucleotide polymorphism.

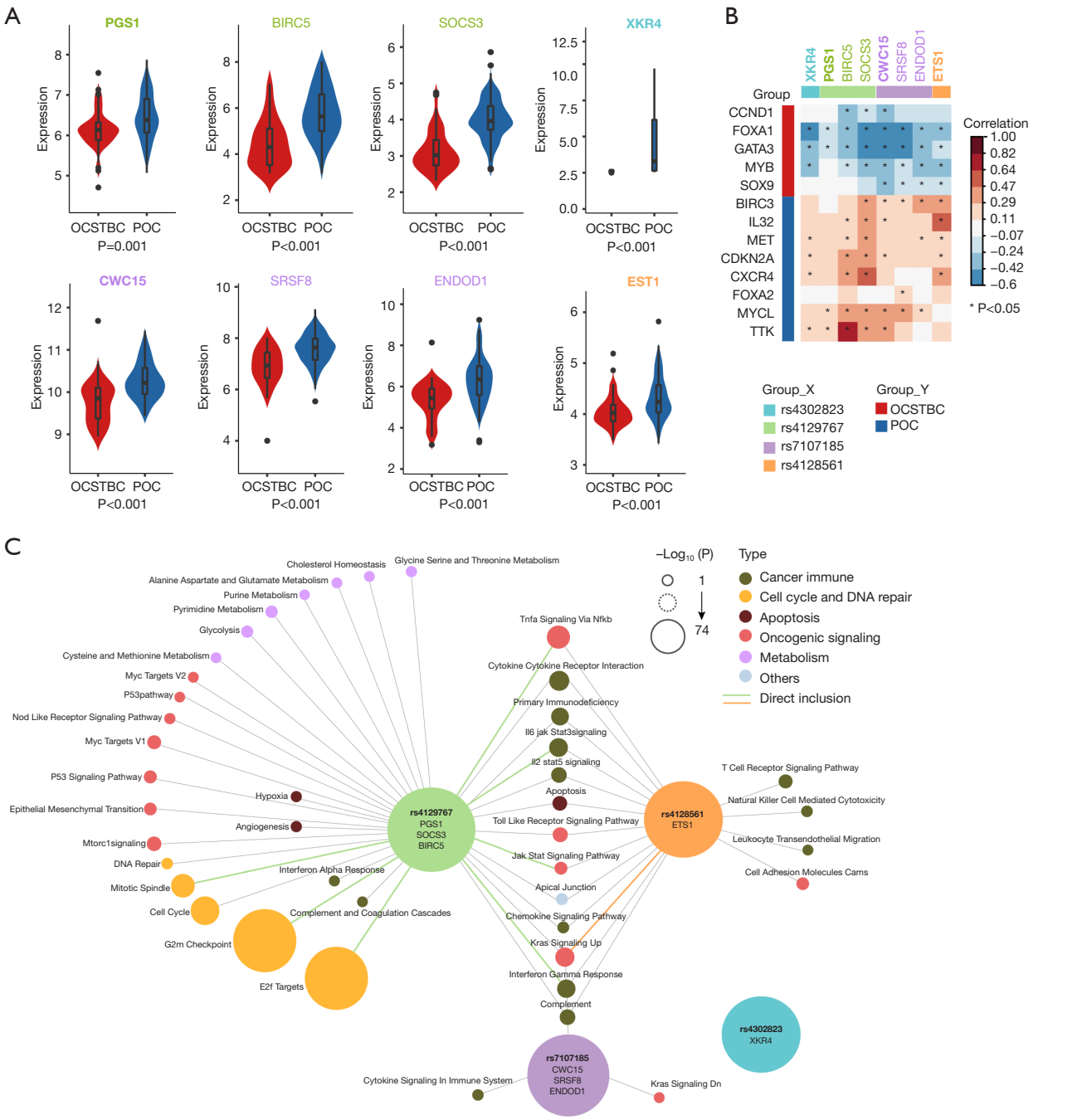

Figure 6 Transcriptome expression of candidate genes. (A) Genome candidate genes are differentially expressed in the transcriptome. Candidate genes were within 200 kb upstream and downstream of 4 SNPs. Candidate genes corresponding to different SNPs have names with different colors. The name of the gene where SNP is located is in bold. (B) Correlations between 8 candidate genes (columns) and 13 key genes (rows) of the transcriptome. (C) Enrichment results of candidate genes for 4 SNPs. The size of the pathway's circle represents the significance of the enrichment [$-\log_{10}$(P value)], and the color represents the pathway type. The colored lines indicate that the pathway directly contains candidate genes, and the gray lines indicate that the pathway is enriched by the related genes of the candidate genes. POC, primary ovarian cancer; OCSTBC, ovarian cancer secondary to breast cancer; SNP, single nucleotide polymorphism.

clinical practice.

In our exploration of the immune environment of POC and OCSTBC, we found that most of the immune cells with a high degree of infiltration in POC are protective against ovarian cancer, such as $CD3^+$ T cells, $CD8^+$ T cells, cytotoxic lymphocytes, myeloid dendritic cells, and M1 macrophages. However, M2 macrophages showed a different behavior from the other immune cells, which were more enriched in OCSTBC. Tumor-associated macrophage (TAM) is one of the major types of immune cells, and M2 polarization of TAM plays a positive role in regulating tumor growth, migration, and angiogenesis by leading to the production of growth factors and cytokines by macrophages (49). Many studies in recent years have demonstrated the interaction between tumors and macrophages in the metastatic microenvironment. M2 macrophages promote metastasis of gastric and breast cancer cells by secreting *CHI3L* (50). Hypoxic epithelial ovarian cancer-derived exosome miR-940 promotes proliferation and migration of epithelial ovarian cancer through induction of macrophage M2 polarization (51). MiR-934 induces M2 polarization in human macrophages to promote liver metastasis from colorectal cancer (52). Moreover, M2 infiltration has been significantly associated with large tumor size and angiogenesis in breast cancer (43). In conclusion, these data suggested that tumor cells might have a reconstituted immune-related TME and M2 macrophages promote the metastasis of breast tumor cells to the ovary.

After analyzing the SNP typing data, we mapped four novel susceptibility loci associated with the POC/OCSTBC phenotype: rs7107185, rs4128561, rs4302823, and rs4129767. Among them, two variant sites, rs7107185 and rs4128561, had relatively high effect sizes (OR >28). Most of these two variant sites are T/T in OCSTBC, but C/C in POC. Combining the transcriptome to study the functional role of variant sites in regulating gene expression, it was found that the expression of genes (*XKR4*, *CWC15*, *PGS1*, *ETS1*) where these mutation sites were located was also different in the transcriptome. Therefore, we believe that these variant loci and genes have the discriminative power of POC and OCSTBC.

However, such an approach may be biased because of heterogeneity among tumor cells with respect to the expression of particular markers. Our profiling did not rely on a tumor cell selection process but rather on the clinical classification which was informative with respect to tumor cell enrichment and correlation with biological characteristics. Another limitation of this study is that the validation analysis should be further confirmed in prospective cohorts. However, these discoveries should be verified with bio-experimentation.

Conclusions

In this study, we determined new biomarkers to distinguish POC and OCSTBC. Furthermore, we described the panorama of POC and OCSTBC in the transcriptome, immune-omics, and genomics, enriching the understanding of the biological characteristics of the two types of ovarian cancer.

Acknowledgments

None.

Footnote

Reporting Checklist: The authors have completed the STREGA reporting checklist. Available at https://tcr.amegroups.com/article/view/10.21037/tcr-24-1441/rc

Peer Review File: Available at https://tcr.amegroups.com/article/view/10.21037/tcr-24-1441/prf

Funding: This study was supported by National Natural Science Foundation of China (grant No. 62076015).

Conflicts of Interest: All authors have completed the ICMJE uniform disclosure form (available at https://tcr.amegroups.com/article/view/10.21037/tcr-24-1441/coif). The authors have no conflicts of interest to declare.

Ethical Statement: The authors are accountable for all aspects of the work in ensuring that questions related to the accuracy or integrity of any part of the work are appropriately investigated and resolved. The study was conducted in accordance with the Declaration of Helsinki (as revised in 2013).

References

1. Webb PM, Jordan SJ. Global epidemiology of epithelial ovarian cancer. Nat Rev Clin Oncol 2024;21:389-400.
2. Frisbie L, Pressimone C, Dyer E, et al. Carcinoma-associated mesenchymal stem cells promote ovarian cancer heterogeneity and metastasis through mitochondrial transfer. Cell Rep 2024;43:114551.
3. Bayraktar E, Chen S, Corvigno S, et al. Ovarian cancer metastasis: Looking beyond the surface. Cancer Cell 2024;42:1631-6.
4. Kroeger PT Jr, Drapkin R. Pathogenesis and heterogeneity of ovarian cancer. Curr Opin Obstet Gynecol 2017;29:26-34.
5. Murphy B, Miyamoto T, Manning BS, et al. Myeloid activation clears ascites and reveals IL27-dependent regression of metastatic ovarian cancer. J Exp Med 2024;221:e20231967.
6. Kubeček O, Laco J, Špaček J, et al. The pathogenesis, diagnosis, and management of metastatic tumors to the ovary: a comprehensive review. Clin Exp Metastasis 2017;34:295-307.
7. Wilson AL, Moffitt LR, Doran BR, et al. Leader cells promote immunosuppression to drive ovarian cancer progression in vivo. Cell Rep 2024;43:114979.
8. Guerriero S, Alcazar JL, Pascual MA, et al. Preoperative diagnosis of metastatic ovarian cancer is related to origin of primary tumor. Ultrasound Obstet Gynecol 2012;39:581-6.
9. Tian W, Zhou Y, Wu M, et al. Ovarian metastasis from breast cancer: a comprehensive review. Clin Transl Oncol 2019;21:819-27.
10. Zheng G, Baandrup L, Wang J, et al. Ovarian cancer risk factors in relation to family history. J Natl Cancer Inst 2024;116:1767-74.
11. Wei X, Sun L, Slade E, et al. Cost-Effectiveness of Gene-Specific Prevention Strategies for Ovarian and Breast Cancer. JAMA Netw Open 2024;7:e2355324.
12. Yu P, Hu C, Ding G, et al. Mutation characteristics and molecular evolution of ovarian metastasis from gastric cancer and potential biomarkers for paclitaxel treatment. Nat Commun 2024;15:3771.
13. Lewis F, Beirne J, Henderson B, et al. Unravelling the biological and clinical challenges of circulating tumour cells in epithelial ovarian carcinoma. Cancer Lett 2024;605:217279.
14. Bergstrom EN, Abbasi A, Díaz-Gay M, et al. Deep Learning Artificial Intelligence Predicts Homologous Recombination Deficiency and Platinum Response From Histologic Slides. J Clin Oncol 2024;42:3550-60.
15. Tserkezoglou A, Kontou S, Hadjieleftheriou G, et al. Primary and metastatic ovarian cancer in patients with prior breast carcinoma. Pre-operative markers and treatment results. Anticancer Res 2006;26:2339-44.
16. van Dam PA, van Dam PJ, Verkinderen L, et al. Robotic-assisted laparoscopic cytoreductive surgery for lobular carcinoma of the breast metastatic to the ovaries. J Minim Invasive Gynecol 2007;14:746-9.
17. Antila R, Jalkanen J, Heikinheimo O. Comparison of secondary and primary ovarian malignancies reveals differences in their pre- and perioperative characteristics. Gynecol Oncol 2006;101:97-101.
18. Lin XY, Zhou XJ, Yang SP, et al. Pseudo-Meigs' syndrome secondary to breast cancer with ovarian metastasis: a case report and literature review. Front Oncol 2023;13:1091956.
19. Cerkauskaite D, Zilinskas K, Varnelis P, et al. Ovarian metastases from breast cancer: A report of 24 cases. J Gynecol Obstet Hum Reprod 2021;50:102075.
20. Bigorie V, Morice P, Duvillard P, et al. Ovarian metastases from breast cancer: report of 29 cases. Cancer 2010;116:799-804.
21. Nesic K, Krais JJ, Wang Y, et al. BRCA1 secondary splice-site mutations drive exon-skipping and PARP inhibitor resistance. Mol Cancer 2024;23:158.
22. Zhu Y, Pei X, Novaj A, et al. Large-scale copy number alterations are enriched for synthetic viability in BRCA1/BRCA2 tumors. Genome Med 2024;16:108.
23. Rezoug Z, Totten SP, Szlachtycz D, et al. Universal Genetic Testing for Newly Diagnosed Invasive Breast Cancer. JAMA Netw Open 2024;7:e2431427.
24. Tanaka Y, Amano T, Nakamura A, et al. Rapamycin prevents cyclophosphamide-induced ovarian follicular loss and potentially inhibits tumour proliferation in a breast cancer xenograft mouse model. Hum Reprod 2024. [Epub ahead of print]. doi: 10.1093/humrep/deae085.
25. Meyniel JP, Cottu PH, Decraene C, et al. A genomic and transcriptomic approach for a differential diagnosis between primary and secondary ovarian carcinomas in patients with a previous history of breast cancer. BMC

Cancer 2010;10:222.
26. Lili LN, Matyunina LV, Walker LD, et al. Molecular profiling predicts the existence of two functionally distinct classes of ovarian cancer stroma. Biomed Res Int 2013;2013:846387.
27. Ritchie ME, Phipson B, Wu D, et al. limma powers differential expression analyses for RNA-sequencing and microarray studies. Nucleic Acids Res 2015;43:e47.
28. Subramanian A, Tamayo P, Mootha VK, et al. Gene set enrichment analysis: a knowledge-based approach for interpreting genome-wide expression profiles. Proc Natl Acad Sci U S A 2005;102:15545-50.
29. Becht E, Giraldo NA, Lacroix L, et al. Estimating the population abundance of tissue-infiltrating immune and stromal cell populations using gene expression. Genome Biol 2016;17:218.
30. Newman AM, Steen CB, Liu CL, et al. Determining cell type abundance and expression from bulk tissues with digital cytometry. Nat Biotechnol 2019;37:773-82.
31. Purcell S, Neale B, Todd-Brown K, et al. PLINK: a tool set for whole-genome association and population-based linkage analyses. Am J Hum Genet 2007;81:559-75.
32. Turner SD. qqman: an R package for visualizing GWAS results using Q-Q and manhattan plots. Biorxiv 2014. doi: 10.1101/005165.
33. Shin JH, Blay S, Mcneney B, et al. LDheatmap: An R Function for Graphical Display of Pairwise Linkage Disequilibria between Single Nucleotide Polymorphisms. Journal of Statistical Software 2006;16:c03.
34. Boughton AP, Welch RP, Flickinger M, et al. LocusZoom.js: interactive and embeddable visualization of genetic association study results. Bioinformatics 2021;37:3017-8.
35. Hänzelmann S, Castelo R, Guinney J. GSVA: gene set variation analysis for microarray and RNA-seq data. BMC Bioinformatics 2013;14:7.
36. Otasek D, Morris JH, Bouças J, et al. Cytoscape Automation: empowering workflow-based network analysis. Genome Biol 2019;20:185.
37. Song P, Li Y, Dong Y, et al. Estrogen receptor β inhibits breast cancer cells migration and invasion through CLDN6-mediated autophagy. J Exp Clin Cancer Res 2019;38:354.
38. Yang F, Xie HY, Yang LF, et al. Stabilization of MORC2 by estrogen and antiestrogens through GPER1-PRKACA-CMA pathway contributes to estrogen-induced proliferation and endocrine resistance of breast cancer cells. Autophagy 2020;16:1061-76.
39. Samimi G, Ring BZ, Ross DT, et al. TLE3 expression is associated with sensitivity to taxane treatment in ovarian carcinoma. Cancer Epidemiol Biomarkers Prev 2012;21:273-9.
40. Kashiwagi S, Fukushima W, Asano Y, et al. Identification of predictive markers of the therapeutic effect of eribulin chemotherapy for locally advanced or metastatic breast cancer. BMC Cancer 2017;17:604.
41. Jayasingam SD, Citartan M, Thang TH, et al. Evaluating the Polarization of Tumor-Associated Macrophages Into M1 and M2 Phenotypes in Human Cancer Tissue: Technicalities and Challenges in Routine Clinical Practice. Front Oncol 2019;9:1512.
42. Pan Y, Yu Y, Wang X, et al. Tumor-Associated Macrophages in Tumor Immunity. Front Immunol 2020;11:583084.
43. Jeong H, Hwang I, Kang SH, et al. Tumor-Associated Macrophages as Potential Prognostic Biomarkers of Invasive Breast Cancer. J Breast Cancer 2019;22:38-51.
44. Mantovani A, Allavena P. The interaction of anticancer therapies with tumor-associated macrophages. J Exp Med 2015;212:435-45.
45. Nabeki B, Ishigami S, Uchikado Y, et al. Interleukin-32 expression and Treg infiltration in esophageal squamous cell carcinoma. Anticancer Res 2015;35:2941-7.
46. Liu Y, Carlsson R, Comabella M, et al. FoxA1 directs the lineage and immunosuppressive properties of a novel regulatory T cell population in EAE and MS. Nat Med 2014;20:272-82.
47. Davis DG, Siddiqui MT, Oprea-Ilies G, et al. GATA-3 and FOXA1 expression is useful to differentiate breast carcinoma from other carcinomas. Hum Pathol 2016;47:26-31.
48. Espinosa I, Gallardo A, D'Angelo E, et al. Simultaneous carcinomas of the breast and ovary: utility of Pax-8, WT-1, and GATA3 for distinguishing independent primary tumors from metastases. Int J Gynecol Pathol 2015;34:257-65.
49. Franklin RA, Liao W, Sarkar A, et al. The cellular and molecular origin of tumor-associated macrophages. Science 2014;344:921-5.
50. Chen Y, Zhang S, Wang Q, et al. Tumor-recruited M2 macrophages promote gastric and breast cancer metastasis via M2 macrophage-secreted CHI3L1 protein. J Hematol Oncol 2017;10:36.
51. Chen X, Ying X, Wang X, et al. Exosomes derived from hypoxic epithelial ovarian cancer deliver microRNA-940

to induce macrophage M2 polarization. Oncol Rep 2017;38:522-8.
52. Zhao S, Mi Y, Guan B, et al. Tumor-derived exosomal miR-934 induces macrophage M2 polarization to promote liver metastasis of colorectal cancer. J Hematol Oncol 2020;13:156.

Cite this article as: Long J, Liu B, Li J, Ji X, Zhu N, Zhuang X, Wang H, Li L, Chen Y, Li X, Zhao S. Comprehensive analysis of molecular characteristics between primary and breast-derived metastatic ovarian cancer. Transl Cancer Res 2025;14(3):1675-1690. doi: 10.21037/tcr-24-1441